Robust and Adaptive Scheduling of Sequential Periodic Sensing for Cognitive Radios

Qiang Liu, *Student Member, IEEE,* Xin Wang, *Member, IEEE,* and Yong Cui, *Member, IEEE*

***Abstract*—Spectrum sensing is a crucial element of dynamic spectrum access (DSA) as it enables cognitive radios (CRs) to opportunistically access the under-utilized spectrum. Existing efforts on sensing have not adequately addressed sensing scheduling over time for better detection performance. In this work, we consider sequential periodic sensing of an in-band channel. We focus primarily on finding the appropriate sensing frequency during an SU's active data transmission on a licensed channel. Detection schemes addressing channel state change and anomalous data are designed specifically to facilitate short-term sensing adaptation to the variations in sensed data. In addition, long-term adaptation is also considered so that the evolving sensing environment can be reflected in the sensing schedule as well. Simulation results demonstrate that our design guarantees better conformity to the spectrum access policies by significantly reducing the delay in change detection while ensuring better sensing accuracy.**

***Index Terms*—Cognitive radio, sequential periodic spectrum sensing, in-band channel, channel detection time, change and outlier detection, sensing adaptation.**

I. Introduction

COGNITIVE radio (CR), a wireless paradigm that aims to access the crowded but under-utilized spectrum more efficiently, has attracted surging interests in recent years. In CR, unlicensed secondary users (SUs) detect the presence/absence of licensed primary users (PUs) via spectrum sensing. Sensing is enforced by the CR system primarily to protect the PUs against excessive interferences from the SUs, but it also helps the SUs seek better spectrum opportunities for their own data transmission. Although sensing is crucial for CR, the ultimate goal of any SU is to have a higher data rate for its own communications. Therefore, it is always desirable that the SUs achieve efficient sensing by reducing resource consumption (e.g., energy, time) while meeting certain system requirements (delay, accuracy, etc.).

Existing studies on the networking aspect of the dynamic spectrum access [17] have generally focused on developing algorithms to use the spare spectrum while assuming that the available channels have been detected or can be easily detected with minimal time and/or without errors. On the other hand, many studies from the signal processing communities have applied sophisticated detection techniques [17] with the assumption that the SU has perfect knowledge of the primary users' signal features and the available channels can be used continuously. There has been very limited research effort on sensing scheduling over time, a significant issue in secondary spectrum access because it directly pertains to the extent the SUs can make use of the available spectrum opportunities while bringing minimal interference to the communications among the licensed channel users.

CR sensing is often not one-time detection; an SU should check the channel status *periodically* even during its data transmission. Although some PUs do exhibit long-term statistical patterns, many wireless devices are subject to unpredictable ON-OFF switching and mobility. A PU of the latter type can reclaim its channel at any time, demanding timely evacuation of the SU therein. Such uncertainty in the PUs necessitates periodic sensing of the channels by the SUs with robust online decision-making algorithms. Another core element of this work is a *sequential* detector that accumulates data gradually over time till a certain decision threshold is reached. Applying sequential detection is particularly suited to the periodicity of the sensing process, where sensing takes place within a time frame that resembles a moving window, a structure that facilitates the SU to schedule its sensing action over time.

We address sensing of the *in-band* channel which an SU is using for its own data transmission. The quality of this channel is the paramount issue for an SU during its data transmission. Instead of studying how cooperation can potentially benefit the sensing performance [12], we are primarily interested in the extent to which different scheduling schemes of one single SU affect its sensing performance. This often reflects the scenarios with limited resources, such as the unavailability of the nearby SUs or insufficient battery power of an SU that prevents it from participating in cooperation.

If the channel status changes during sensing (e.g., when a PU returns), an SU should take extra care so that it could vacate the channel faster. The competing requirements on the maximum protection of the PU and channel utilization of the SU lead us to design an adaptive scheduling scheme, in which the SU dispenses more sensing efforts whenever "signs" of a possible PU return are observed. Meanwhile, sensing should be robust against possible data outliers, whose effect may sometimes resemble that of the real channel state change and may lead to a wrong sensing decision. A heuristic algorithm is proposed to spot and exclude such extreme measurements. Because of the channel variations and uncertainties in a real system, a sensing schedule should be updated to reflect any long-term shift in the environment. Since it is

Manuscript received April 1, 2013; revised August 15, 2013. A preliminary version of this paper has been included in the Proc. 32nd IEEE International Conference on Computer Communications (INFOCOM 2013), Turin, Italy.

Q. Liu and X. Wang are with the Department of Electrical and Computer Engineering, Stony Brook University, Stony Brook, NY, 11794 (e-mail: {qiangliu, xwang}@ece.sunysb.edu).

Y. Cui is with Tsinghua University, Beijing, P. R. China (e-mail: cuiyong@tsinghua.edu.cn).

Digital Object Identifier 10.1109/JSAC.2014.1403003.

in general unrealistic to directly measure the instantaneous channel signal-to-noise ratio (SNR), an SU should observe the shift in the statistics of its sensed data and allow gradual and periodic adaptation to reflect such changes. We consider an adaptive schedule over time that utilizes certain properties of the underlying sequential detection algorithm.

The major contributions of this work are as follows:

- We introduce the *Grouped-Data Sequential Probability Ratio Test* (GD-SPRT) as the baseline sequential detection scheme for our periodic sensing, in which grouping effectively reduces the impact of short-term channel randomness;
- We explore the timing issues during the periodic sensing, and propose a sensing schedule according to the average speed of the underlying sequential test;
- We propose short-term change and outlier detection schemes for robust decision making with the presence of anomalous data as well as prompt detection of a channel state change so that the PUs can be effectively protected against prolonged interference;
- We design an online adaptive scheduling algorithm, which updates the sensing frequency based on the detected change in the sequentially observed sensing data;
- We provide simulation results to demonstrate the validity and major advantages of our design.

The rest of the paper is organized as follows. After presenting related works in Sec. II, we provide an overview of the sensing preliminaries and the system model in Sec. III. Next in Sec. IV, we discuss the baseline sequential detection rule. In Sec. V, focusing on long-term sensing scheduling, we propose our scheme based on the average run speed of the sequential test; this is further developed in Sec. VI, which addresses short-term change and outlier detection. In Sec. VII, an adaptive algorithm is proposed that accounts for the changes in the sequentially observed data. Simulation results and their analysis can be found in Sec. VIII before we conclude the paper in Sec. IX.

II. Related Work

Among the numerous studies on spectrum sensing, very few have considered periodic in-band channel sensing. We found [7] and [11] are closest to our work. In [7], a deterministic off-line scheme is proposed to find the appropriate sensing frequency. Upon careful examination, the simple OR-rule cannot always guarantee that the prescribed accuracy requirements are met under varying channel conditions. In [11], the authors use Wald's sequential test, a well-known sequential detector, to accumulate groups of data within a predefined period and make a final decision. Although at first glance our sensing scheme looks similar, fundamental differences exist in the ways sensing is scheduled, data are accumulated, and the decisions are made over time. On the other hand, works such as [2], [3], and [18] have considered reward-based scheduling schemes and their optimality, but it's unclear how these algorithms can be applied in practical systems.

Some studies, such as [4] and [9], have considered change detection for cognitive radios. By utilizing the cumulative sum (CUSUM) approaches, they aim to find the theoretically quickest detector – in a single test – in the wake of a channel state change without considering how such tests can be scheduled over time. On the other hand, outlier detection has not been systematically studied for CR applications. In this work, we focus primarily on practical implementations of the change and outlier detection rules in order to satisfy the specific requirements for periodic sensing. Parameter adaptation is a viable approach in dynamic system design; however, very little has been studied about sensing adaptation in the context of cognitive radio. Attention has been given to the somewhat more passive threshold adaptation during the detection process such as in [5] and [16]; we, on the other hand, are more interested in the adaptation of sensing actions carried out by the SUs, which is a more effective means to proactively tackle the system variation and uncertainty.

In our earlier work [10], we performed initial studies on sequential periodic sensing. In this work, we provide more detailed analysis on its implementation and proofs on certain properties of the detector. In addition, we introduce a long-term adaptation algorithm to account for the variation and uncertainty in the environment. Finally, we have performed more extensive performance evaluation and analysis to demonstrate the effectiveness of our proposed algorithms in balancing the dual requirements of PU protection and SU channel access.

III. Sensing Preliminaries and System Model

For an in-band channel currently being used by an SU, the two hypotheses regarding the state of the channel are as follows:

- H_0: The channel is still available (the PU is absent);
- H_1: The channel is occupied by the PU.

1) Sensing Method: If an SU has enough knowledge about the PU signal characteristics, it can apply feature detection, which often yields more accurate sensing decisions. For example, the cyclostationary feature of an ATSC DTV signal has been used for detection of the pilot signals [7], [8]. In contrast, an energy detector measures only the intensity of the ambient signal without relying on any prior information about the PU signal features. Energy detection generally runs much faster than feature detection, at the cost of reduced accuracy. In our study, no prior knowledge about the PU signal features is assumed; the general form of the energy detection serves as the building block for our sequential detection.

2) Noise and Signal Powers: Every SU in the network is equipped with a single transceiver so that sensing and data communication cannot coincide. The local noise level follows a wide-sense-stationary (WSS) process, whose average power has been calibrated as σ^2. If the current in-band channel has been sensed during the PU's earlier "ON" periods, the SU may have measured and recorded the actual signal power, from which the long-term average can be calculated. Subtracting the calibrated noise power from this average, the SU can coarsely estimate the average received signal power from the associated PU alone.

In a real system, the scattering environment, interference, and mobility may subject the average received signal power to various degrees of fluctuation. It's also not always possible for

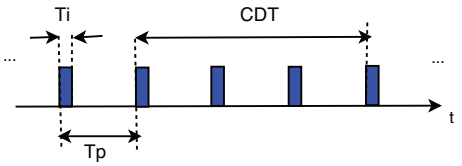

Fig. 1. Channel detection time CDT, sensing period T_p, and sensing time T_i

the SU to pinpoint the source of the electromagnetic energy it receives. Any signal, if strong enough beyond the calibrated local noise, is detrimental to the SU's data transmission. Regardless of the actual signal source – the PU or other interferers – the SU should aim to detect the presence of any external signals, and switch to another channel for its data transmission if the intensity becomes strong enough. The SU can define a target signal level P for the detection task, which is to be used as the *nominal* signal power in our sequential detector.

3) Time Measures in Periodic Sensing: Fig. 1 illustrates the structure of the in-band channel periodic sensing with equally spaced intervals. The channel detection time (CDT) is defined as the maximum allowed time for a sensing decision to be made. A CDT usually consists of multiple sensing-transmission periods, each being called a *sensing period* T_p; and the continuous portion within each T_p dedicated to sensing is the *sensing time* T_i. We have $T_p \leq CDT$ so that the channel is sensed at least once during a CDT period with a sensing decision subsequently being made. We note that the CDT is particularly the requirement in IEEE WRAN 802.22, a standard for opportunistic use of the TV-band white spaces [1].

Because the SU is often bound by hardware constraints so that it can only take a fixed number of samples at a time. In this work, the value of T_i is given as 1 ms [7], while the length of T_p can be changed, which reflects variable sensing schedules. Likewise, due to many higher-layer concerns such as coordination and synchronization, often only a set of discrete T_p values are allowed in a practical system. For example, in 802.22 WRAN, T_p may only take values that are multiples of a MAC frame size 10 ms. In this work, sensing scheduling is equated with choosing an appropriate T_p, and the final step of "discretizing" the value will be implicitly assumed. The *sensing overhead* describes the proportion of time dedicated to the sensing task and is defined as the ratio between T_i and T_p. In this work, T_i (1 ms) is rather short compared to T_p ($k \cdot 10$ ms), and the sensing overhead is at most 10% for satisfactory secondary data communication performance.

IV. Grouped-data Sequential Probability Ratio Test (GD-SPRT)

A sequential detector observes data over time and decides, at each step, whether the set of observations it has collected is sufficiently reliable for decision making; and if yes, which underlying hypothesis is acting to yield the observed data. Both a stopping rule and a decision rule are in place for sequential detection. The parametric version of the sequential detection is applied in our study, where the noise and nominal PU signal power levels are used as input parameters.

Wald's Sequential Probability Ratio Test (SPRT) [14] is a well-known sequential detection scheme. The SPRT accumulates the log-likelihood ratio of the i.i.d. individual samples till either of the two constant thresholds is reached. It has been proved that for one run of the detector, on average, Wald's SPRT needs the fewest samples among all the tests for the same (P_{FA}, P_{MD}) requirement. Here P_{FA} and P_{MD} denote false alarm and missed detection probabilities, respectively. In this work, we also adopt an SPRT-like detection scheme, namely, the *grouped-data SPRT* (GD-SPRT), with data samples within each T_i being grouped together to form a "super-sample". This can reduce the effect of short-term channel randomness (e.g., multi-path fading) which exists on a much smaller timescale (i.e., in the microseconds) compared to T_i.

Step 1: Calculate the energy $y(\mathbf{x})$ from M samples.

The SU collects the ambient signal at a certain sampling rate. After a sensing block T_i, the energy of M samples contained within is

$$y(\mathbf{x}) = \sum_{i=1}^{M} x_i^2, \tag{1}$$

where x_i denotes the individual samples within T_i.

In practice, the number of samples taken within a single T_i is fairly large. For example, for $T_i = 1$ ms, $M = 6,000$ with the Nyquist sampling rate of a 6 MHz TV band. With the law of large number approximation ($M \gg 10$), we have

$$y(\mathbf{x}) \overset{i.i.d.}{\sim} \begin{cases} H_0 : \mathcal{N}(MP_n, MP_n^2), \\ H_1 : \mathcal{N}(MP_n(1+SNR), MP_n^2(1+SNR)^2), \end{cases} \tag{2}$$

which can be easily obtained from the results in [13]. Here, SNR is defined as the ratio between the nominal signal power P and local noise floor $\sigma^2 = P_n B$, where P_n is the noise power spectral density (PSD) and B is the channel bandwidth. An energy sample of duration T_i is approximately Gaussian regardless of the original distribution of the PU signal.

Step 2: Derive the test statistic $T(y(\mathbf{x}))$ for each group.

The log-likelihood ratio (LLR) of the energy sample is calculated as

$$T(y(\mathbf{x})) = \ln \frac{f_1(y(\mathbf{x}))}{f_0(y(\mathbf{x}))}, \tag{3}$$

where $f_0(\cdot)$ and $f_1(\cdot)$ are the pdfs under H_0 and H_1, respectively, as indicated in Eq. (2). Since the energy sample $y(\mathbf{x})$ is the data that we will be directly handling, for ease of exposition, from now on, we will simply refer to $y(\mathbf{x})$ as y.

Step 3: Accumulate the test statistics $T(y)$ across groups to obtain the aggregate test statistic $\mathcal{T}$, and compare it against two constant thresholds A and B.

Each T from Step 2 corresponds to one group of data. For the n-th group, we have

$$T(y_n) = \ln \frac{f_1(y_n)}{f_0(y_n)}. \tag{4}$$

As we accumulate T's sequentially, the aggregate test statistic up to the n-th group is

$$\mathcal{T}_n = \sum_{k=1}^{n} T(y_k) = \sum_{k=1}^{n} \ln \frac{f_1(y_k)}{f_0(y_k)}. \tag{5}$$

The two decision thresholds are chosen the same values as those in Wald's SPRT:

$$A = \ln \frac{p_{MD}}{1-p_{FA}}, \text{ and } B = \ln \frac{1-p_{MD}}{p_{FA}}. \tag{6}$$

The decision rule for the SU is

- if $\mathcal{T}_n > B$, it decides that the PU has reclaimed the channel;
- if $\mathcal{T}_n < A$, it decides that the channel is still available;
- otherwise, it continues to sample another group of data and update $\mathcal{T}_{n+1}$ using Eq. (5).

The *stopping time* N is defined as the minimum number of steps after which one of the two decision thresholds is first crossed; that is,

$$N = \min\{n : \text{ either } \mathcal{T}_n < A \text{ or } \mathcal{T}_n > B\}. \tag{7}$$

V. Sensing Scheduling in Sequential Periodic Sensing

The SU should find an appropriate spectrum sensing schedule so that requirements for protecting the PU can be satisfied while the spectrum, once available, is utilized to the best extent by the SU. In this section, we provide analysis on the long-term scheduling of the sequential test, which serves as the foundation of our short-term adaptive sensing design.

A. Average Increment, Run Length, and Overhead

For the baseline sequential detector introduced earlier, we consider the expected values of the test statistics, the average run steps and the average sensing overhead.

Proposition V.1. *Each of the i.i.d. test statistics $T(y)$ has the expected values*

$$\begin{aligned} m_0 &\triangleq \mathbb{E}[T(y)|H_0] \\ &= -\frac{M-1}{2}\frac{SNR^2}{(1+SNR)^2} + \frac{SNR}{(1+SNR)^2} - \ln(1+SNR), \end{aligned} \tag{8}$$

and

$$\begin{aligned} m_1 &\triangleq \mathbb{E}[T(y)|H_1] \\ &= \frac{M+1}{2} SNR^2 + SNR - \ln(1+SNR), \end{aligned} \tag{9}$$

under H_0 and H_1, respectively.

Proof: Let μ_0, μ_1, σ_0, and σ_1 be the means and variances indicated by Eq. (2). Using the identity $\mathbb{E}[x^2] = \text{Var}[x] + (\mathbb{E}[x])^2$, we can easily obtain

$$\mathbb{E}[(y-\mu_0)^2|H_0] = \sigma_0^2; \tag{10}$$

$$\mathbb{E}[(y-\mu_1)^2|H_0] = \sigma_0^2 + (\mu_1-\mu_0)^2; \tag{11}$$

$$\mathbb{E}[(y-\mu_1)^2|H_1] = \sigma_1^2; \tag{12}$$

$$\mathbb{E}[(y-\mu_0)^2|H_1] = \sigma_1^2 + (\mu_1-\mu_0)^2. \tag{13}$$

Since

$$\begin{aligned} T(y) &= \ln \frac{f_1(y)}{f_0(y)} \\ &= \ln \frac{\frac{1}{\sqrt{2\pi}\sigma_1} \exp -\frac{(y-\mu_1)^2}{2\sigma_1^2}}{\frac{1}{\sqrt{2\pi}\sigma_0} \exp -\frac{(y-\mu_0)^2}{2\sigma_0^2}} \\ &= \ln \frac{\sigma_0}{\sigma_1} - \left(\frac{(y-\mu_1)^2}{2\sigma_1^2} - \frac{(y-\mu_0)^2}{2\sigma_0^2} \right), \end{aligned} \tag{14}$$

we have

$$\begin{aligned} m_0 &= \mathbb{E}[T(y)|H_0] \\ &= \ln \frac{\sigma_0}{\sigma_1} - \frac{\sigma_0^2 \mathbb{E}[(y-\mu_1)^2|H_0] - \sigma_1^2 \mathbb{E}[(y-\mu_0)^2|H_0]}{2\sigma_0^2\sigma_1^2} \end{aligned} \tag{15}$$

$$= \ln \frac{\sigma_0}{\sigma_1} - \frac{\sigma_0^2(\sigma_0^2 + (\mu_1-\mu_0)^2) - \sigma_1^2\sigma_0^2}{2\sigma_0^2\sigma_1^2} \tag{16}$$

$$\begin{aligned} &= \ln \frac{\sigma_0}{\sigma_1} + \frac{\sigma_1^2 - \sigma_0^2 + (\mu_1-\mu_0)^2}{2\sigma_1^2} \\ &= \frac{1}{2} \ln \frac{MN^2}{MN^2(1+SNR)^2} \\ &+ \frac{MN^2(1+SNR)^2 - MN^2 + (MN(1+SNR) - MN)^2}{2MN^2(1+SNR)^2} \\ &= -\ln(1+SNR) + \frac{SNR}{(1+SNR)^2} - \frac{M-1}{2}\frac{SNR^2}{(1+SNR)^2}, \end{aligned}$$

which is Eq. (8).

We can similarly derive m_1. The only difference is that the conditional expectations to be plugged into Eqs. (15) and (16) are replaced by Eqs. (12) and (13). ■

The above m_0 and m_1 are the average increments at each step of the sequential test. We first note that for the same M, both values depend solely on SNR. The average speed of the sequential test has a direct bearing on the separation of the two underlying distributions. In fact, thanks to the independence of different sample groups, Eq. (8) is the opposite of the Kullback-Leibler (KL) information number [6]:

$$-I_{01} = \mathbb{E}\left[\ln \frac{f_1(T)}{f_0(T)} | H_0 \right] = \int f_0(u) \ln \frac{f_1(u)}{f_0(u)} \, \mathrm{d}u. \tag{17}$$

Intuitively, as the SNR increases, the KL distance becomes farther apart, and the two hypotheses can be faster distinguished from one another.

By plotting both m_0 and m_1 under variable SNR values, we observe that $|m_0| < |m_1|$ and both $|m_0|$ and $|m_1|$ increase monotonically with SNR. With low channel SNRs, that is, $SNR \to 0^+$, we have $1 + SNR \approx 1$ and $\ln(1+SNR) \approx SNR$. Plugging these two equations into Eqs. (8) and (9), we have

$$m_0 \approx -\frac{M}{2} SNR^2, \text{ and } m_1 \approx \frac{M}{2} SNR^2. \tag{18}$$

That is, the absolute values of the average increments under H_0 and H_1 are roughly the same when the channel SNR is low; in other words, the underlying sequential test runs at the same rate under both hypotheses.

In general, the exact distribution of the test statistic is difficult to derive; however, when the SNR is low, the distributions under H_0 and H_1 can be approximated as Gaussian, as shown below.

Proposition V.2. *Under low-SNR conditions, we have*

$$T(y) \overset{i.i.d.}{\sim} \begin{cases} H_0 : \mathcal{N}(m_0, 2m_1), \\ H_1 : \mathcal{N}(m_1, 2m_1), \end{cases} \tag{19}$$

in which m_0 and m_1 are given in Eq. (18)*.*

Proof: In our settings, the relative standard deviation (RSD), defined as the ratio between the standard deviation and the absolute value of the mean, is fairly small with large M values. From Eq. (2), the RSDs under both distributions are $1/\sqrt{M}$. The difference between σ_0 and σ_1 is hence much smaller than that between μ_0 and μ_1 and can be ignored.

Now in Eq. (14), if $\sigma_0 = \sigma_1$, we have

$$\begin{aligned} T(y) &= -\frac{(y-\mu_1)^2 - (y-\mu_0)^2}{2\sigma_0^2} \\ &= \frac{\mu_1 - \mu_0}{\sigma_0^2} y - \frac{\mu_1^2 - \mu_0^2}{2\sigma_0^2}. \end{aligned} \tag{20}$$

Recall that if $x \sim \mathcal{N}(\mu, \sigma^2)$, then $ax + b \sim \mathcal{N}(a\mu + b, a^2\sigma^2)$. Here $a = \frac{\mu_1 - \mu_0}{\sigma_0^2}$ and $b = -\frac{\mu_1^2 - \mu_0^2}{2\sigma_0^2}$, and then

$$T(y) \sim \begin{cases} H_0 : \mathcal{N}(-\frac{(\mu_1-\mu_0)^2}{2\sigma_0^2}, \frac{(\mu_1-\mu_0)^2}{\sigma_0^2}), \\ H_1 : \mathcal{N}(\frac{(\mu_1-\mu_0)^2}{2\sigma_0^2}, \frac{(\mu_1-\mu_0)^2}{\sigma_0^2}). \end{cases} \tag{21}$$

From Eq. (2), we finally have

$$T(y) \sim \begin{cases} H_0 : \mathcal{N}(-\frac{M}{2} SNR^2, M * SNR^2), \\ H_1 : \mathcal{N}(\frac{M}{2} SNR^2, M * SNR^2), \end{cases} \tag{22}$$

which is Eq. (19). ∎

From Eq. (19), the test statistics under H_0 and H_1 are symmetric around zero: they have equal variances and opposite means. This means it would take, on average, the same number of steps for a sequential test to hit either the lower or upper decision boundary.

Next we consider the average run length – the average number of sample groups that need to be collected in order to reach either decision threshold.

Proposition V.3. *Regardless of the SNR value, the average run lengths for the SU to make a decision on the channel state under H_0 and H_1 are*

$$\mathbb{E}[N|H_0] = \frac{p_{FA}B + (1 - p_{FA})A}{m_0} \tag{23}$$

and

$$\mathbb{E}[N|H_1] = \frac{(1 - p_{MD})B + p_{MD}A}{m_1} \tag{24}$$

respectively.

Proof: The aggregate test statistic $\mathcal{T}$ under either hypothesis satisfies

$$\mathbb{E}[\mathcal{T}_N|H_k] = \mathbb{E}[T_N|H_k] * \mathbb{E}[N|H_k], \ k = 0, 1. \tag{25}$$

If after N steps, $\mathcal{T}_N$ happens to cross a decision threshold under H_0, then with probability $1 - P_{FA}$, the lower boundary $A = \ln \frac{P_{MD}}{1-P_{FA}}$ is crossed; and with probability P_{FA}, the upper boundary $B = \ln \frac{1-P_{MD}}{P_{FA}}$ is crossed. Ignoring the effect of overshooting beyond the thresholds, the expected value of $\mathbb{E}[\mathcal{T}_N|H_0]$ can then be found as

$$\mathbb{E}[\mathcal{T}_N|H_0] = (1 - P_{FA})A + P_{FA}B. \tag{26}$$

Since $m_0 = \mathbb{E}[T_N|H_0]$, from Eq. (25), we have

$$\mathbb{E}[N|H_0] = \frac{(1 - P_{FA})A + P_{FA}B}{m_0}. \tag{27}$$

And $\mathbb{E}[N|H_1]$ can be found similarly. ∎

From Eqs. (6), (23), and (24), when $P_{FA} = P_{MD}$, we have $A + B = 0$ and $\mathbb{E}[N|H_0] = \mathbb{E}[N|H_1]$. That is, the sequential test has a symmetric structure and it takes an equal number of steps on average to reach either decision boundary. Had more stringent requirement been imposed on P_{MD} to ensure minimal interference to the PUs, that is, $P_{MD} \ll P_{FA}$, we would have $|A| >> |B| \approx -\ln P_{FA}$. In this case, even with nearly identical increments $|m_0| = |m_1|$ when the channel SNR is very low, the upper threshold takes much less time to be crossed so that when the PU is indeed present, the SU is expected to quickly make the correct decision.

From Eqs. (18), (23), and (24), the expected numbers of samples for running one sequential test under H_0 and H_1 with low channel SNRs are

$$M * \mathbb{E}[N|H_0] \approx -\frac{2\left((1 - P_{FA})A + P_{FA}B\right)}{SNR^2} \tag{28}$$

and

$$M * \mathbb{E}[N|H_1] \approx \frac{2\left((1 - P_{MD})B + P_{MD}A\right)}{SNR^2} \tag{29}$$

respectively.

If both Eqs. (28) and (29) are multiplied by the sampling period – the inverse of the sampling frequency – then we have the total expected time spent on sensing. For a given time frame for the detection task, say CDT, the expected sensing overhead ρ under both hypotheses can also be obtained:

$$\mathbb{E}[\rho|H_0] = T_i/CDT * \mathbb{E}[N|H_0], \tag{30}$$

$$\mathbb{E}[\rho|H_1] = T_i/CDT * \mathbb{E}[N|H_1]. \tag{31}$$

To summarize the results in this subsection, for a single run of the GD-SPRT, we have the following relationships: For a given channel SNR value, the number of samples M and the expected run length $\mathbb{E}[N]$ are inversely proportional under either hypothesis; as such, the expected sensing overhead $\mathbb{E}[\rho|H_0]$ and $\mathbb{E}[\rho|H_1]$ are fixed. The overhead under each hypothesis is in turn proportional to SNR^{-2}. If the channel SNR is reduced by 5 dB, for instance, the average number of samples required to maintain the same sensing accuracy level would be 10 times the original. Since in our settings, T_i always takes a preset value, the expected run length of the sequential test would assume such a change.

B. Sensing Scheduling Based on the Average Run Steps of the Sequential Test

So far we have considered only a single sequential test without the context of scheduling it over time. If the conventional GD-SPRT is applied over time for periodic sensing of the in-band channel, the sensing process would have a structure shown in Fig. 2 (a). Time is divided into non-overlapping

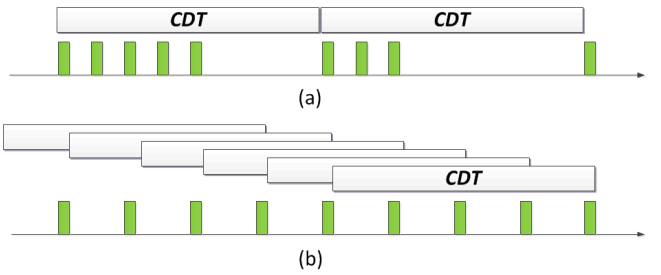

Fig. 2. Sensing scheduling with (a) forward, non-overlapping GD-SPRT and (b) backward, overlapping GD-SPRT

units, each with length CDT. The standard GD-SPRT runs within each window till either threshold is crossed. As long as an H_0 decision is made, the rest of the CDT period is dedicated to uninterrupted secondary data transmission. The scheme proposed in [11] has the very same structure; in particular, the maximum allowable run steps N_{max} is used for the initial sensing period: $T_p^{'} = CDT/N_{max}$. Normally, N_{max} is fairly large; and with moderate SNR levels, most of the sensing action would usually have ended well before the end of a CDT period.

We aim to design a different sensing strategy, in which sensing is scheduled according to the average running speed of the underlying sequential test and the sample groups are taken uniformly across a CDT-window. In contrast to the earlier scheme, in which only one sensing decision is made for every non-overlapping CDT period, in our design, after collecting new sensing data after every T_p, the SU updates its sensing decision. As such, we let the CDT-window slide forward by T_p after a new group of data has been collected[1], as shown in Fig. 2 (b).

Different from the conventional GD-SPRT, in our design, as the CDT-window moves forward, a GD-SPRT runs *backward* at each position of the CDT-window, starting from the latest group of data. Since the newest data within the current window might be generated from a different distribution from the older ones, by having each sequential test run backward, we reduce any impact of the older sensing data in the CDT-window that might obscure the effect of the newer ones so that a possible state change can be detected earlier.

We have the expected run lengths to make a sensing decision – either right or wrong – under hypotheses H_0 and H_1 as in Eqs. (23) and (24). However, for scheduling, we consider using the expected number of steps under the condition that the "correct" decision threshold is crossed (e.g., the lower boundary A under H_0). Let this number be denoted as $N_A = A/m_0$, then the sensing period is determined by

$$\begin{aligned} T_p &= \min\{T_{p,A}, T_{p,B}\} \\ &= \min\{\frac{CDT}{N_A}, \frac{CDT}{N_B}\} \\ &= \min\{\frac{CDT}{A/m_0}, \frac{CDT}{B/m_1}\} = \frac{CDT}{A} m_0, \end{aligned} \tag{32}$$

[1]Although it seems that much higher computational effort is needed, this is hardly the case. As one newly collected data group moves inside the CDT-window, an old group at the end moves out; only the net change – the difference between the two associated test statistics – needs to be calculated.

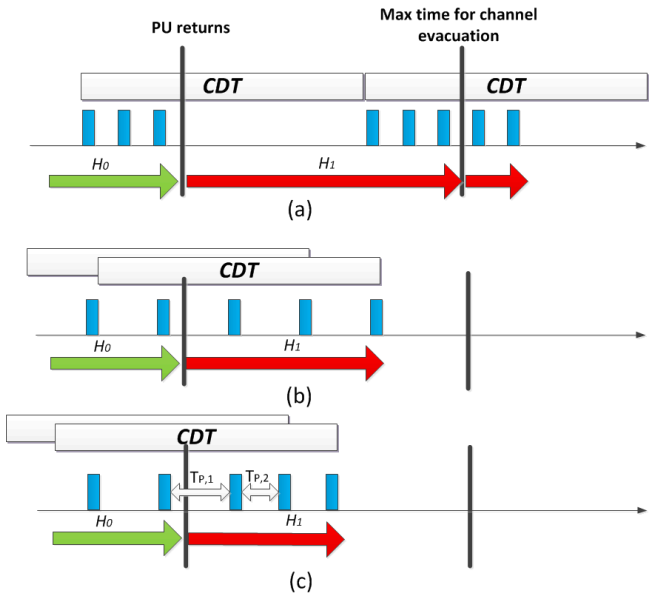

Fig. 3. Detection delay (indicated by the red arrows) with (a) forward, non-overlapping GD-SPRT; (b) backward, overlapping GD-SPRT; and (c) backward, overlapping GD-SPRT with short-term T_p adjustment

in which $N_B = B/m_1$ is similarly defined for the other scenario where the SU expects to reach B under H_1; $T_{p,A} = CDT/N_A$ and $T_{p,B} = CDT/N_B$ are the sensing periods, in order to reach A and B respectively when test statistics are taken uniformly within the CDT-window. Finally, we take the minimum of the two so that under both hypotheses the CDT-window contains at least the average number of test statistics to reach the correct decision threshold. The last equation holds because $|m_0| < |m_1|$, and $|A| \geq |B|$ when $P_{MD} \leq P_{FA}$. This also agrees with the fact that the SU is currently sensing its in-band channel, and hence H_0 should be considered as the "default" condition.

Both the conventional and our scheme described above are illustrated in Fig. 3. Here, the PU returns right after the sensing action ended in one of the non-overlapping CDT periods. In (a), as the channel goes undetected until the next window, the evacuation delay of the SU may exceed the required length CDT, thereby violating the system requirement. On the other hand, in (b), the returning PU might be detected earlier before the evacuation deadline, thanks to the closer intervals between adjacent sensing groups. In (c), further actions are taken by the SU, where the sensing frequency is increased after a possible PU return is suspected, which results in even faster channel evacuation. We defer the detailed design of this change detection to Sec. VI.

Due to randomness in the GD-SPRT, the SU may not have made a sensing decision by the time it has used up all the data within the CDT-window. Since each test is run backward starting from the newly collected sensing data, when more data are needed, the SU may have to go beyond the CDT-window and retrieve historical data to continue running the test. This again demonstrates the flexibility of our backward-running GD-SPRT. Another issue is that if a test does not run to completion, regardless of the length of the historical data retrieved, the test should be truncated after the final step. A

sequential test can easily be truncated in the end by reducing the distance between the two decision thresholds A and B to zero.

VI. Dynamic Change and Outlier Detections

This section addresses both the detection of the "turning point", where the channel state shifts from H_0 to H_1 due to PU return, and the anomalous data (i.e., outliers) encountered during sensing that could easily lead to a wrong sensing decision. We aim to improve the sensing quality for the in-band channel by "adaptation" of sensing actions over a much finer timescale within CDT; whereas the adaptation to be introduced in the next section occurs over a longer period of time, usually several to tens of CDT.

A. Change Detection for the In-Band Channel

In an ideal scenario, following a different distribution, newly sensed data would exhibit an abrupt shift in some manner from the older ones. Unfortunately, this is not the case under low channel SNR levels, as the test statistics under both distributions are so close that a large proportion of test statistics under H_0 end up near the average of H_1. However, by accumulating data over time, the SU might be able to gather evidence that shows (1) a sufficient amount of data have shifted from an earlier level and (2) the shift is consistent, thereby declaring a channel state change. This is the underlying theme for all change detectors; still, the challenge here is that the SU is only allowed up to CDT time to observe this consistent change from the time instant the PU reclaims the channel.

We design a short-term adjustment mechanism so that (1) the SU can immediately elevate its sensing action – by increasing its sensing frequency – when a possible channel state change is first suspected; and (2) the SU reverts to its default sensing frequency if the aforementioned consistent shift is not observed within a certain amount of time. Hence, our change detection consists of two stages, the first one being the regular "check", and the second elevated sensing action after the SU has raised its "alert level" due to suspicion of a possible state change.

1) Triggering the Elevated Sensing Action: With the sequential periodic sensing structure in place, our change detector has the following features. Similar to that in the regular sequential detection in our design, in the change detection, the test statistics are again accumulated backward. On the other hand, since the channel state change must be detected within CDT, the data used in our change-detection come only from within the CDT-window; that is, no earlier historical data are retrieved for change detection. The following algorithm is applied:

$$\mathcal{T}_c = \max\{\bar{m}_{new} - \bar{m}_{old}\} \geq \delta, \tag{33}$$

in which $\mathcal{T}_c$ is the change-point test statistic; $\bar{m}_{new}$ and $\bar{m}_{old}$ are averages of the newer and older test statistics in the CDT-window respectively; and δ is a system-defined threshold that determines the sensitivity of the SU to the shift. With larger δ values, the SU is less sensitive to the changes in the observed data.

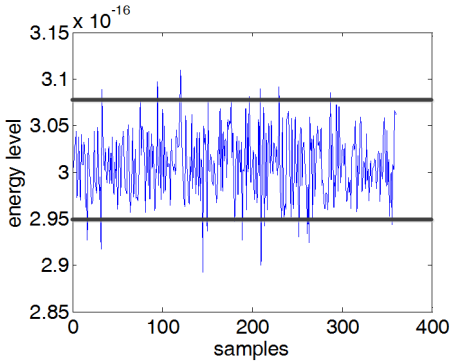

Fig. 4. Outlier detection: Two thresholds are used to identify outliers

For the given set of test statistics in the CDT-window, the SU starts with the most recent group of data (with the remaining in the window as "old") and calculates the difference; hereafter, the new and old data lengths are increased and decreased by one respectively till Eq. (33) is first satisfied. At this point, the second-stage elevated sensing is triggered. This feature is in sharp contrast with the conventional change schemes, where a change is immediately declared following a threshold being crossed. In our scenario, the low channel SNR means the SU might be very susceptible to false alarms as well if it is too sensitive to the changes. Our two-stage design thus aims to balance the performance requirements of quick detection of change versus higher detection accuracy.

2) Elevated Sensing: There are many ways to schedule the elevated sensing. Two main issues of concern here are the sensing frequency and decision-making frequency. While the former is self-explanatory, the second factor means whether a decision should be made every time a new sample group is taken, even with the increased sensing frequency. The goal is to detect a change as quickly as possible while not incurring too much sensing overhead. The easiest way to bypass these concerns would be to schedule maximum sensing with a decision being made every FS, namely, the smallest possible T_p. Although its accuracy performance is expected the best among all the options, the computation load can become very high, with the sensing overhead reaching the maximum, thereby obviating the very need for efficient sensing scheduling in the first place. A few options are studied in our subsequent simulation section that demonstrate the trade-offs among performance metrics.

B. Outlier Detection

Unlike a real channel state change due to the arrival/departure of the PU use, the outliers could stem from variable sources, such as environmental abnormalities (thunderstorms, electric spark, etc.), the internal hardware miscalibration that results in wrong measurements, or simply due to extreme channel variation such as short-term deep fading or strong interferences. Due to the cumulative nature of the sequential test, a single outlier could affect multiple adjacent tests containing it, for instance, by slowing them down and increasing the detection delay significantly. Therefore, these rare but extreme observations should be spotted quickly and excluded from the decision-making process.

In a dynamic environment, the only way a single SU might be able to spot possible extreme data is to compare with the "norm" in a largely statistical sense. In Fig. 4, a snapshot of the energy samples taken during sensing is plotted. Two thresholds are used to exclude the few samples that are farther away from the majority. In our context, it is easier to handle the processed test statistic that is distributed close to zero, and hence the general rule for a new test statistic T_{new} is

$$\eta_1 \leq T_{new} < \eta_2, \tag{34}$$

where the $\eta_1 < 0 < \eta_2$ are the two thresholds.

Numerous methods exist in the statistics literature that deal with how to identify outliers. We apply one of the most popular methods that is based on the interquartile range [15]. If Q_1 and Q_3 are the lower and upper quartiles (i.e., 25% and 75% of the rank statistics) of the recent data respectively, then one could define an outlier to be any observation outside the range $[Q_1 - K * (Q_3 - Q_1), Q_3 + K * (Q_3 - Q_1)]$ for some positive constant K. Once an outlier is identified, it again can be handled in more than one way. For example, the SU can ignore the sample and retake another one immediately afterward for replacement. Alternatively, the excess portion of the outlier can be removed and thus the outlier is "rounded" to η_1 or η_2, which is named "winsorization" in the literature [15]. In our performance studies, we consider different K values and their impact on the detection performance when the perceived outliers are simply discarded.

VII. Sensing Adaptation for Sequential Periodic Sensing

In a dynamic system, channel uncertainties, such as interference, noise fluctuation, and fading, may complicate the detection process and compromise the expected detection performance. The SU should measure the long-term statistics of its observed sensing data and adaptively update its sensing parameters so that the new schedule can better meet the requirements for PU protection and SU channel utilization.

In this work, we consider the desired P_{FA} or P_{MD} value as the adaptation target; and in our performance studies, we set $P_{FA} = P_{MD} \triangleq P^* = 0.1$. Since it is impossible for the SU to obtain its *actual* P_{FA} and P_{MD} values on the go[2], we consider the prospective online accuracy performance via the *virtual threshold* determined by the actual data – the average of the aggregate test statistics within the CDT-window – and reversely calculate the corresponding false-alarm and missed-detection probabilities[3].

We let p_v denote the *virtual probability* of sensing errors by reversely applying Eq. (6), that is,

$$P_v = \{P : |thre|_v = \ln \frac{1-P}{P}\}, \tag{35}$$

where $|thre|_v$ is the average of the aggregate test statistic within the CDT-window. Subsequently, we define

$$r_v = \frac{P_v - P^*}{P^*} \tag{36}$$

as the expected rate of change from P_v toward the target P^*. Then the general adaptation rule for the sensing period T_p is

$$T_{p,new} = \max\left(T_p^{min}, \min(T_p^{max}, T_{p,old} + \alpha N_c r_v)\right) \tag{37}$$

In the equation, $T_{p,old}$ and $T_{p,new}$ denote the T_p values before and after adaptation, respectively. T_p^{min} and T_p^{max} are respectively the minimum and maximum allowable T_p values. N_c is the change in the number of FSs, that corresponds to unit rate of change in P_v (i.e., $r_v = 1$). The parameter $\alpha \in (0, 1)$ is a damping factor that controls the level of adaptation. As α gets closer to one, the sensing period would almost immediately be adjusted to the intended new value, which could easily incur oscillatory adjustments as the difference between the virtual and target error rates might be inflated due to randomness and/or extreme observations. With a smaller α, any adaptation step toward the target is carried out more gradually, and further actions are pending on observations to be collected in the future. For example, suppose from the recently sensed data, the SU calculates $P_v = 0.2$, namely, $r_v = 1$; then from Eq. (37), we find the intended one-time reduction of T_p equals 10 FS's if $N_c = 10$. The SU may instead choose to reduce T_p by 5 FS's, following $\alpha = 0.5$.

Due to the randomness of the energy samples, the averages of the aggregate test statistics for the calculation of P_v and r_v may fluctuate over time when an insufficient number of samples are taken. Therefore, the averages should be calculated over a longer timescale than that of the CDT-window, for example, at most once every 10 seconds. Another factor that should be taken into account is the average duration of the environmental changes, such as that of the channel shadow fading due to slow-moving obstacles nearby, or that of the interfering signals in the channel. The random nature of these events again may decide the adaptation frequency or the adaptation factor α during a particular time period is not optimal.

Another important aspect of sensing adaptation is its frequency. Similar to our earlier argument on adaptation levels, the SU should refrain from over-frequent adjustments of its sensing parameters so that the process can be run with relative stability. However, the adaptive sensing should also keep pace with the change in channel statistics if the system is more dynamic.

Despite their different goals, the regular, change, and outlier detection processes are integrated into a single framework in our adaptive sequential periodic sensing design. During regular sensing, as a new energy sample is taken, the test statistic is calculated and the outlier detection is first run. With a valid test statistic, the change-point detection is run using all the data within the current CDT-window, and the resulting action depends on whether the elevated sensing is triggered. If not, regular sensing is performed (that can utilize earlier historical data); otherwise, elevated sensing is run till either an H_0 or H_1 decision is made and the sensing period is reset to the original level. On a much longer time scale, long-term adaptation is carried out so that any changes in the environment are accounted for in the form of adjusted sensing frequency. Because of this integrated framework, a change of one factor (such as any of the thresholds) would result in

[2]In fact the SU is not always able to retroactively determine the correctness of its earlier decisions.

[3]For simplicity of exposition, we only present analysis here when the two target error probabilities are equal. Otherwise, the problem can be a bit more complicated but can be solved as a bivariate problem.

TABLE I
DEFAULT SENSING SCHEDULING UNDER VARIABLE PU SIGNAL LEVELS

PU energy level (dBm)	-119	-118	-117	-116	-115	-114
Tp/FS	5	7	12	19	29	46

variations of multiple performance metrics. Such effects will be studied in detail in the performance evaluation section.

VIII. PERFORMANCE EVALUATION

In this section, we conduct MATLAB simulation studies to demonstrate the performance of our design. In particular, we consider the following performance metrics: the sensing overhead and error probability[4] during regular detection under H_0; and change detection delay and failure probability during change detection. These two detection scenarios are specifically distinguished from one another so that we can show the trade-offs between their requirements. In addition, sensing adaptation is studied in the context of interference.

A. Simulation Setup

1) System Parameters: We study the IEEE 802.22 WRAN environment with a single primary transmitter and a secondary user located at the edge of the keep-out radius [1]. The channel detection time $CDT = 2$ s while the required $P_{FA} = P_{MD} = 0.1$. The commonly used noise power is $\sigma^2 = P_n B = -95.2$ dBm, in which the noise floor PSD $P_n = -163$ dBm/Hz and B is the DTV channel bandwidth 6 MHz. The default signal strength P for the DTV signal detection threshold at the keep-out radius is -116 dBm (corresponding to $SNR = -20.8$ dB) [13], and unless otherwise specified, a range of SNR values will be subsequently studied to demonstrate the effect of different sensing schedules.

2) Detection Parameters: We use the interquartile range (IQR) outlier detector with the default $K = 1.5$. The change detection is triggered when the default δ, twice the running average of the recent test statistics, is first crossed. The two thresholds A and B as in Eq. (6) are used for regular detection, with up to 3 s of data (i.e., data within the 2 s CDT-window and extra ones from 1 s prior to the window) for retrieval. The truncation threshold at the last step is zero if no decision is made by crossing either A or B.

B. Performance and Analysis

First, Table I lists the default normalized T_p values (with respect to the MAC frame size FS) under a range of PU signal levels as determined by Eq. (32).

1) Elevated Sensing Action: Echoing the discussions in Sec. VI-A2, we tested the sensing performance under different options in the second stage of the change detection, i.e., elevated sensing, listed in Table II.

From the table, we can see the two schemes "conv" and "sched0" have been introduced and conceptually compared with each other in Sec. V-B. The remaining schemes differ by how sensing and decision-making periods are selected. In the schemes "sched1" and "sched2", the elevated sensing period T_p^{elev} is immediately reduced to a certain pre-determined value, but no decision is made until the original scheduled T_p time is reached; in other words, the elevated sensing only serves to provide more data. In contrast, "sched3" and "sched4" see the elevated sensing periods reduced to one half and one third of the original respectively, while a sensing decision is made every time with the arrival of a new group of sample.

TABLE II
ELEVATED SENSING SCHEDULING FOR COMPARISON

notation	explanation
"conv"	non-overlapping CDT, forward GD-SPRT (Sec. V-B or [11])
"sched0"	moving-CDT, backward GD-SPRT w/o change detection
"sched1"	–, $T_p^{elev} \leftarrow 5FS$, no decision till next T_p
"sched2"	–, $T_p^{elev} \leftarrow 2FS$, no decision till next T_p
"sched3"	–, $T_p^{elev} \leftarrow T_p/2$, with immediate decisions
"sched4"	–, $T_p^{elev} \leftarrow T_p/3$, with immediate decisions

In Figs. 5 and 6, the regular and change detection performances are respectively plotted under these variable elevated sensing actions. From Fig. 5, the sensing overhead of "conv" is indeed very close to that of "sched0", as we demonstrated in Sec. V that the overhead is a function of total number of samples. However, even with $1.5CDT$ length of data, the regular sensing error probability $P_{FA} = P_{MD}$ is still above the target value 0.1. Thanks to elevated sensing in all other schemes, this error performance is improved to varying degrees, at the cost of extra sensing overhead; nevertheless, the overhead is still well below the maximum 10%. Among the schemes, again, we observe the trade-offs between overhead and sensing error performances. For instance, if the sensing period is reduced immediately to $2FS$, as in "sched2", for higher PU energy levels (say, at -116 dBm), much higher overhead is incurred compared to other options, so is better sensing accuracy.

More drastic effects of applying elevated sensing can be observed in Fig. 6. Under low PU signal levels, the average detection time for the channel state change, across all the cases with elevated sensing, is reduced by more than 50%, compared to that under "conv" and "sched0"; and the resulting detection failure probability – defined as the probability that the change has not been detected CDT time after the PU's return – is also much smaller, often below 1%. In addition, the trend in the change detection failure probability is the same as that in the average detection delay; as the average delay goes up, the PU will have a less chance to have been detected by the deadline.

Interestingly, the change detection time and failure probability follow different trends for "conv" and all other schemes. For "conv", which doesn't have a separate change detection mechanism, as the channel SNR degrades, each round of forward detection on average takes longer time, which in turn means that more likely the PU will return in the middle of a test when the decision on the channel state has not been

[4]Since our focus is on the in-band channel sensing, this error is P_{FA}. But had the underlying distribution been H_1, the results for P_{MD} are very close to the ones shown here.

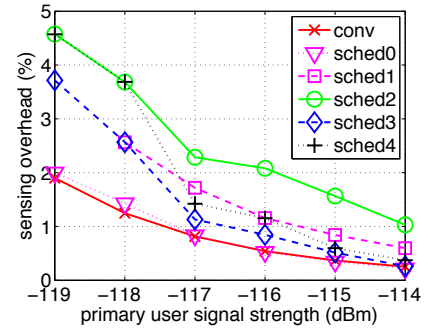

(a)

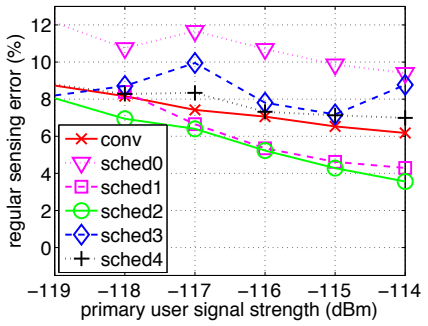

(b)

Fig. 5. Regular detection: (a) overhead and (b) probability of sensing error with variable elevated sensing actions

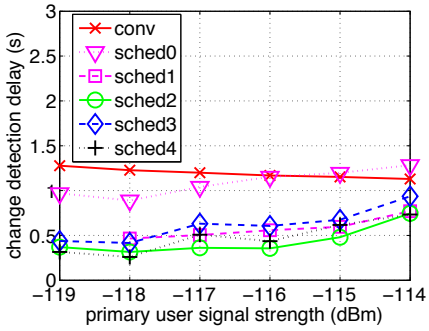

(a)

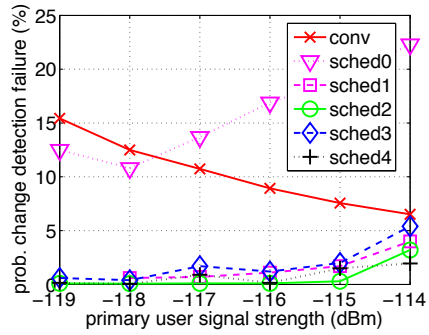

(b)

Fig. 6. Change detection: (a) detection delay and (b) probability of detection failure with variable elevated sensing actions

made[5]. In general, the ongoing test must first "cancels out" the previously accumulated H_0 values before proceeding to reach the other threshold B. As such, the change detection time is much longer. On the other hand, the change detection performance in our design is constrained by the existing interval between adjacent sensing (i.e., the default T_p). With higher SNRs, this interval is larger (see Table I) which introduces a higher initial delay before the SU responds by triggering the elevated sensing.

2) Elevated Sensing Triggering Threshold: In Figs. 7 and 8, the same set of performance metrics under regular and change detections are plotted, with variable thresholds to trigger the elevated sensing. Our subsequent simulation studies use the "sched4" scheme described earlier. The three schemes labeled as "change-thre1", "change-thre2", and "change-thre3" correspond to the cases when the change threshold δ is chosen to be 3x, 2x (default), or 1x of the the recent test statistic averages. The earlier "sched0" scheme without change detection is also shown as "no change" for performance comparison.

From the plots, we observe that as the sensitivity of the SU to change is increased (corresponding to a decreasing δ), both regular and change detection accuracy levels are improved as well, again, at the cost of more sensing effort to dispense. The performance differences among the three schemes are actually not significant, compared to the huge improvement over the baseline scheme without change detection. Therefore, scheduling change detection is beneficial to the regular detection as well since the extra sensing effort is likely to expedite the decision-making process by leading the sequential test out of the intermediate zone between the thresholds A and B faster.

3) Effects of Outliers: We explore different ways to identify the outliers for the same set of data. In Fig. 9, different performance metrics are measured under variable K for the IQR outlier method with the PU signal level set at -116 dBm. The three options labeled as "1", "2", and "3" have $K = 1$, 1.5 (default), and ∞ (no outlier detection), respectively. As K gets smaller, the SU becomes more intolerant of the extreme data; the regular detection accuracy improves while that of the change detection worsens. This is because data collected after the change are more likely to be deemed as outliers initially and discarded, leading to an increased time to declare the change and a higher failure rate. During regular detection, though, removal of the extreme data leads to higher accuracy levels as the tests can run more smoothly toward the intended threshold.

4) Effects of Historical Data: Again setting the PU level at -116 dBm, we tested the impact of historical data length on sensing performance. Figs. 10 and 11 depict the scenario without and with change detection respectively. The historical data lengths used in "1", "2", and "3" are respectively 1 s, 1.5 s (default), and 2 s. Without change detection, all performance metrics are fairly sensitive to the length of the historical data. Interestingly, in this case, as the regular detection accuracy is improved by retrieving more data, the change detection performance degrades as the older data are not helpful in determining a change. On the other hand, thanks to elevated sensing in change detection, data beyond the CDT-window are hardly retrieved, leading to uniform performances across all

[5]Even when the gap as shown in Fig. 3(a) on average gets smaller, the extra effort to take more samples to finish an ongoing test still prevails.

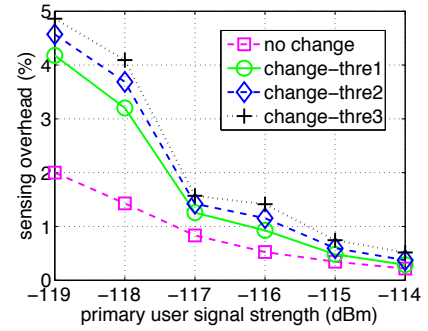

(a)

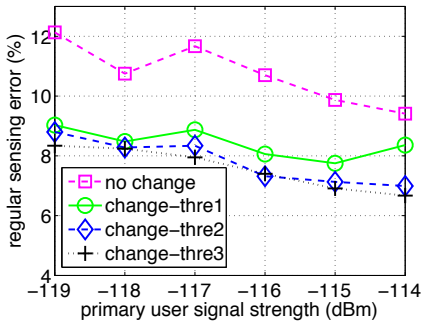

(b)

Fig. 7. Regular detection: (a) overhead and (b) probability of sensing error with variable elevated sensing triggering thresholds

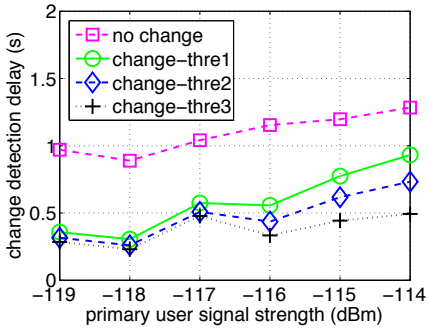

(a)

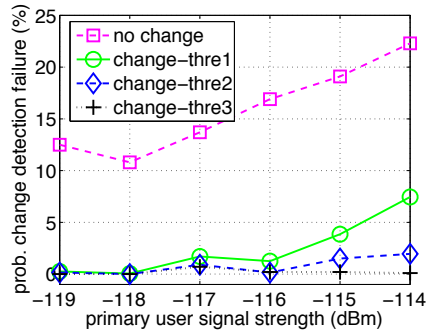

(b)

Fig. 8. Change detection: (a) detection delay and (b) probability of detection failure with variable elevated sensing triggering thresholds

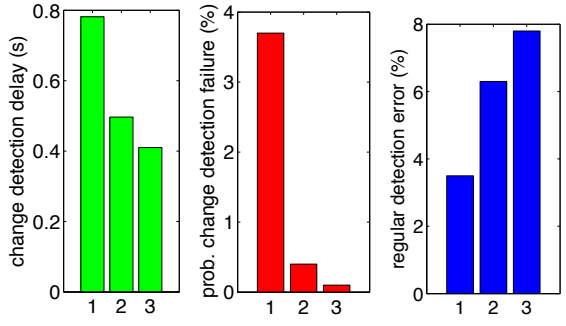

(a) (b) (c)

Fig. 9. Effect of outliers on sensing performance: (a) change detection delay; (b) change failure probability; and (c) regular error probability

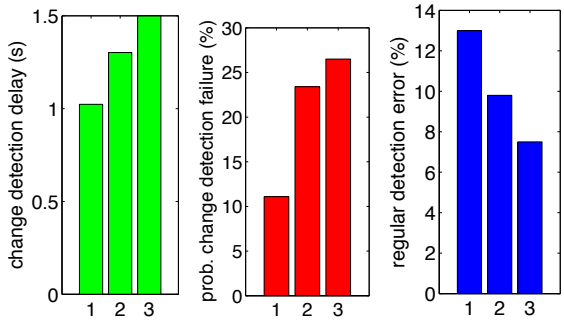

(a) (b) (c)

Fig. 10. Effect of historical data length on sensing performance, no change detection: (a) change detection delay; (b) change failure probability; and (c) regular error probability

the metrics much more superior to the counterparts obtained without change detection.

5) Effects of Adaptation: Finally, we consider the effects of sensing period adaptation algorithm in (37) with variable α values. We consider four test cases, and in each case, an interferer with an average power level P_i set at -125 dBm and -123 dBm is introduced on top of a nominal PU signal level P at -116 dBm. The interferer is present in the network following the Poisson processes with one of the two patterns (1) $\mathbb{E}[\text{ON}] = 10$ s and $\mathbb{E}[\text{OFF}] = 50$ s; and (2) $\mathbb{E}[\text{ON}] = 5$ s and $\mathbb{E}[\text{OFF}] = 55$ s, where "ON" and "OFF" represent the time period where the interference is present and absent respectively. Note that these interference levels are not strong enough to cause excessive performance degradation to the SU access. The sensing performance during H_0 under different conditions is plotted in Fig. 12. Due to interference, the average sensing errors are observed to be above the required 10%.

Intuitively, with an external interference source being superimposed on the existing system, an adaptive sensing schedule calls for more frequent sensing when the interference is present, resulting in higher sensing overhead. This can be observed across the cases shown in Fig. 12(a), as an increasing level of α corresponds to a higher value of overhead. Nevertheless, the increase in overhead is minimal compared to the CDT length. More interestingly, the error performance with increasing α values resembles a V-shaped pattern across all the cases in Fig. 12(b). When α is too small (say, close to

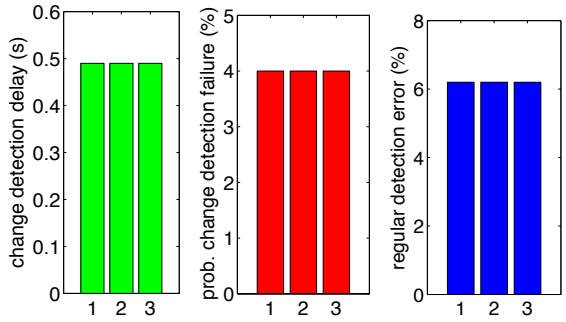

Fig. 11. Effect of historical data length on sensing performance, with change detection: (a) change detection delay; (b) change failure probability; and (c) regular error probability

zero), the adaptation is too slow to accommodate the changing environment. On the other hand, when α is large (e.g., close to one), the adaptation may become so drastic that the sensing frequency swings from one level to another, often crossing multiple FS's. As such, the sensing frequency may get well below the desired level (such as after the interferer disappears), resulting in elevated sensing errors. It is thus more desirable to have "moderate" adaptation levels so that the sensing errors can be controlled in the presence of interference. For example, in the cases shown in the figures, the detection errors without adaptation are anywhere from 10% to 20% higher compared to the adaptive counterparts at $\alpha = 0.5$. As expected, the results in Fig. 12(b) also confirm that the overall sensing performance degrades with increasing magnitudes as well as relative durations of the interference.

C. Discussions

We have explored the trade-offs of detection overhead and accuracy during both regular and change detections. With much higher channel SNRs, the default T_p values may become so large that the benefit of our sequential scheduling is offset by the large initial delay between adjacent groups. On the other hand, when the channel SNR becomes so low that even the "maximum schedule" – with the highest possible sensing frequency – becomes inadequate, an increasing T_i and/or other collaborative SUs may help improve the sensing performance. Besides, long-term sensing adaptation can also be shown to improve the change detection performance with moderate α values, thanks to the largely increased sensing frequency over time.

IX. Conclusion

In this work, we have studied adaptive time-domain scheduling of the in-band sequential periodic spectrum sensing. The system requirements on detection accuracy and delay are highlighted as the guidelines for our sensing scheduling design. Analytical and simulation studies are provided to demonstrate the trade-offs among various performance metrics during sensing. Results show our design guarantees better conformity to the spectrum access policies by significantly reducing the delay in change detection, thus incurring minimal interference to the licensed users, while maintaining

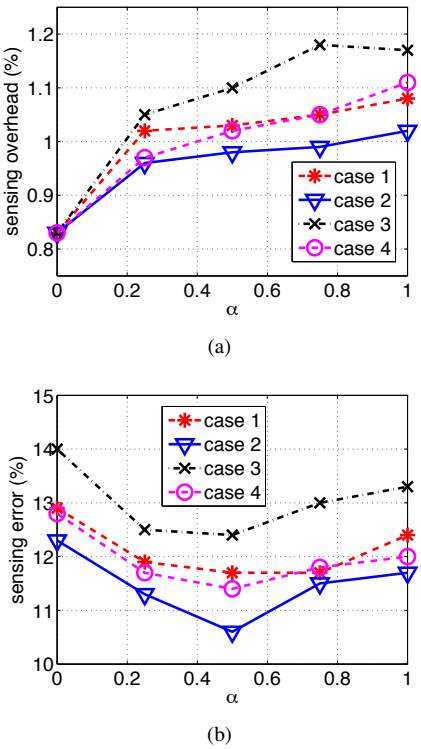

Fig. 12. H_0 detection at the keep-out radius (P = -116 dBm) and maximum stepwise change $N_c = 10$: (a) overhead and (b) probability of sensing error with variable adaptation parameter α: case 1: P_i = -125 dBm, $\mathbb{E}[\text{ON}] = 10$ s, $\mathbb{E}[\text{OFF}] = 50$ s; case 2: P_i = -125 dBm, $\mathbb{E}[\text{ON}] = 5$ s, $\mathbb{E}[\text{OFF}] = 55$ s; case 3: P_i = -123 dBm, $\mathbb{E}[\text{ON}] = 10$ s, $\mathbb{E}[\text{OFF}] = 50$ s; and case 4: P_i = -123 dBm, $\mathbb{E}[\text{ON}] = 5$ s, $\mathbb{E}[\text{OFF}] = 55$ s

desired sensing accuracy. The adaptive design is also shown to increase the resilience of the SU sensing performance in the presence of system interference and uncertainty. Future work may include scheduling for a multi-radio SU as well as the extension of our scheduling to out-of-band channels not currently used by the SU.

Acknowledgment

This research was supported by the US National Science Foundation under grant numbers CNS-1247924 and ECCS-1231800 and was conducted at Stony Brook University.

References

[1] IEEE 802.22 Working Group on Wireless Regional Area Networks. http://www.ieee802.org/22/.

[2] A. T. Hoang and Y. C. Liang. Adaptive scheduling of spectrum sensing periods in cognitive radio networks. In *Proc. IEEE Global Telecommunications Conference, GLOBECOM '07*, pages 3128–3132, Nov. 2007.

[3] S. Huang, X. Liu, and Z. Ding. Optimal sensing-transmission structure for dynamic spectrum access. In *Proc. IEEE INFOCOM 2009*, pages 2295–2303, Apr. 2009.

[4] A. K. Jayaprakasam and V. Sharma. Cooperative robust sequential detection algorithms for spectrum sensing in cognitive radio. In *Ultra Modern Telecommunications Workshops, ICUMT '09. International Conference on*, pages 1 –8, Oct. 2009.

[5] D. R. Joshi, D. C. Popescu, and O. A. Dobre. Dynamic threshold adaptation for spectrum sensing in cognitive radio systems. In *Radio and Wireless Symposium (RWS), 2010 IEEE*, pages 468–471, 2010.

[6] D. Kazakos and P. Papantoni-Kazakos. *Detection and Estimation*. Electrical engineering communications and signal processing series. Computer Science Press, 1990.

[7] H. Kim and K. G. Shin. In-band spectrum sensing in cognitive radio networks: energy detection or feature detection? In *Proc. 14th ACM International Conference on Mobile Computing and Networking (Mobicom '08)*, pages 14–25, 2008.

[8] K. Kim, I. A. Akbar, K. K. Bae, J. Urn, C. M. Spooner, and J. H. Reed. Cyclostationary approaches to signal detection and classification in cognitive radio. In *Proc. IEEE Symposium on New Frontiers in Dynamic Spectrum Access Networks, DySPAN 2007*, pages 212–215, Apr. 2007.

[9] H. Li, C. Li, and H. Dai. Quickest spectrum sensing in cognitive radio. In *Information Sciences and Systems, CISS 2008. Proc. IEEE*, pages 203–208, Mar. 2008.

[10] Q. Liu, X. Wang, and Y. Cui. Scheduling of sequential periodic sensing for cognitive radios. In *Proc. 32nd IEEE International Conference on Computer Communications (INFOCOM 2013)*, pages 2220–2228, Turin, Italy, Apr. 2013.

[11] A. W. Min and K. G. Shin. An optimal sensing framework based on spatial rss-profile in cognitive radio networks. In *Proc. IEEE Conference on Sensor, Mesh and Ad Hoc Communications and Networks, SECON '09*, pages 1–9, Jun. 2009.

[12] S. M. Mishra, A. Sahai, and R. W. Brodersen. Cooperative sensing among cognitive radios. In *Proc. IEEE Conference on Communications, ICC '06*, volume 4, pages 1658–1663, Jun. 2006.

[13] S. J. Shellhammer, S. Shankar, R. Tandra, and J. Tomcik. Performance of power detector sensors of dtv signals in ieee 802.22 wrans. In *Proc. First International Workshop on Technology and Policy for Accessing Spectrum, TAPAS '06*, TAPAS, 2006.

[14] A. Wald. *Sequential Analysis*. John Wiley & Sons., New York, NY, 1947.

[15] R. R. Wilcox. *Introduction to Robust Estimation and Hypothesis Testing, Third Edition*. Academic Press, Waltham, MA, 2012.

[16] T. Yu, S. Rodriguez-Parera, D. Markovic, and D. Cabric. Cognitive radio wideband spectrum sensing using multitap windowing and power detection with threshold adaptation. In *Communications (ICC), 2010 IEEE International Conference on*, pages 1–6, 2010.

[17] T. Yucek and H. Arslan. A survey of spectrum sensing algorithms for cognitive radio applications. *Commun. Surveys Tuts.*, 11(1):116–130, Jan. 2009.

[18] T. Zhang and D. H. K. Tsang. Optimal cooperative sensing scheduling for energy-efficient cognitive radio networks. In *INFOCOM, 2011 Proc. IEEE*, pages 2723 –2731, Apr. 2011.

Qiang Liu is a Ph.D. candidate in the Department of Electrical and Computer engineering at Stony Brook University. His research interests include networked data/information fusion, signal and target detection and estimation, statistical signal processing, wireless sensor networks, as well as spectrum sensing and allocation for cognitive radios.

Xin Wang received the B.S. and M.S. degrees in telecommunications engineering and wireless communications engineering respectively from Beijing University of Posts and Telecommunications, Beijing, China, and the Ph.D. degree in electrical and computer engineering from Columbia University, New York, NY. She is currently an Associate Professor in the Department of Electrical and Computer Engineering of the State University of New York at Stony Brook, Stony Brook, NY. Before joining Stony Brook, she was a Member of Technical Staff in the area of mobile and wireless networking at Bell Labs Research, Lucent Technologies, New Jersey, and an Assistant Professor in the Department of Computer Science and Engineering of the State University of New York at Buffalo, Buffalo, NY. Her research interests include algorithm and protocol design in wireless networks and communications, mobile and distributed computing, as well as networked sensing and detection. She has served in executive committee and technical committee of numerous conferences and funding review panels, and is the referee for many technical journals. She serves as an associate editor of IEEE Transactions on Mobile Computing since 2013. Dr. Wang achieved the NSF career award in 2005 and ONR challenge award in 2010.

Yong Cui received the B.E. degree and the Ph.D. degree from Tsinghua University, China in 1999 and 2004, respectively. He is currently a full professor in Tsinghua University, Council Member in China Communication Standards Association, Co-Chair of IETF IPv6 Transition WG Softwire. Having published more than 100 papers in refereed journals and conferences, he received the National Science and Technology Progress Award of China in 2005, the Influential Invention Award of China Information Industry in both 2012 and 2004, best paper awards in ACM ICUIMC 2011 and WASA 2010. Holding more than 40 patents, he is one of the authors in RFC 5747 and RFC 5565 for his proposal on IPv6 transition technologies. He serves at the Editorial Board on both IEEE TPDS and IEEE TCC. His major research interests include mobile wireless Internet and computer network architecture.